Sławomir Sztajnowski, Izabella Krucińska, *Konrad Sulak, Michał Puchalski, Henryk Wrzosek, Jadwiga Bilska

Lodz University of Technology, Faculty of Material Technologies and Textile Design, Department of Material and Commodity Sciences and Textile Metrology, Centre of Advanced Technologies of Human-Friendly Textiles "Pro Humano Tex"
ul. Żeromskiego 116, 90-924 Łódź Poland,
E-mail: izabella.krucinska@p.lodz.pl

***Institute of Biopolymers and Chemical Fibres,**
ul. M. Sklodowskiej-Curie 19/27, 90-570 Łódź, Poland

Effects of the Artificial Weathering of Biodegradable Spun-Bonded PLA Nonwovens in Respect to their Application in Agriculture

Abstract
The structural changes and mechanical properties of spun-bonded polylactide (PLA) nonwovens resulting from artificial weathering were analyzed in respect to their application in agriculture. The spun-bonded nonwovens were stabilized on a calender at various temperatures ranging from 60 to 110°C. The weathering process was carried out with the use of a Q-SUN weathering chamber under two selected climatic conditions resembling temperate and subtropical climate, respectively. The artificial aging effect on the nonwovens was assessed by measuring their physical parameters and mechanical properties as well as by analyzing their structural changes by means of Fourier infrared spectrophotometry (FTIR), polarization-interference microscopy (PIM) and wide angle X-ray scattering (WAXS).

Key words: *nonwovens, stabilization, structural changes, artificial weathering, mechanical properties.*

Introduction

Biodegradable materials of aliphatic polyesters and copolyesters, owing to their special properties, have been widely used in many fields. At first they were exploited in medicine and pharmacy [1 - 13]. The use of these polymers makes it possible to produce temporary products that after their exploitation are biologically decomposed to nontoxic compounds, disappearing from the environment in a natural way. Therefore they are widely used for agricultural purposes as films and biodegradable and compostable nonwovens [14, 15] for covering plants and subsoils. A spun-bonded nonwoven of poly(lactic acid) (PLA) seems to be a perfect, environmentally friendly product supporting farm production. Its additional advantage is the possibility of processing this biopolymer by means of most standard technologies used in the plastics industry, including thermo-formation, extrusion, injection and blow moldings [16, 17].

The aim of the study was to assess the suitability of spun-bonded PLA nonwovens for agriculture by means of their artificial weathering and to evaluate the effect of calender stabilization parameters on the polymer structural changes and related changes in physical features and mechanical properties [18]. The nonwovens were tested for shrinkage and directional mechanical properties, a parameters that verifies their suitability for agricultural applications.

Test materials

The materials tested were non-modified nonwovens made of PLA6251D (from Nature Works, Japan) by the spun-bonded technique at the Institute of Biopolymers and Chemical Fibers, Łódź, and then followed by calender stabilization. The nonwovens were extruded from the polymer melt on a laboratory stand designed and made by the Research and Development Centre of Textile Machinery 'Polmatex-Cenaro', within the temperature range of 205 - 216 °C, at a rate of 2.2 - 11.0 m/min and a yield ranging from 2.5 to 10.2 kg/h. The nonwovens produced with a surface weight of about 50 g/m^2 (***Table 1***) were thermally stabilized at 65, 70, 85, 90, 100 and 110 °C (±1 °C).

Artificial weathering of nonwovens

The weathering of nonwovens was carried out in a Q-SUN weathering chamber under conditions resembling temperate climate according to standard PN EN ISO 4892-2 based on Technical Report TR 010 ed. May 2004 'Exposure procedure for artificial weathering'. The UV radiation source consisted of three xenon lamps with a total power of 5400 W. The weathering process was performed in cycles, irradiating the nonwovens with a 0.51 W/m^2 UV radiation measured at a wavelength of 340 nm under the following conditions:

- 58 min exposure – BST = 50 °C, ChT = 35 °C, RH = 40%;
- 2 min artificial rainfall with demineralized water and exposure BST = 40 °C, ChT = 25 °C;
- 10 min with no exposure – BST = 30 °C, ChT = 20 °C, RH = 65%; for 14 and 42 h.

The weathering time amounting to 14 h was established on the basis of the change of the forth degree in the blue scale (light fastness test), which corresponds to the natural exposure of a sample during a single summer season, i.e. about 200 h.

The weathering process was carried out to assess the effect of nonwoven irradiation conditions during one season (S1) and three seasons (S3) in temperate climate on the physical properties of nonwovens being essential from the point of view of the foreseen application.

Considering the different shrinkage degrees obtained in tests S1 and S3, it was decided to additionally use exposure conditions resembling subtropical climate – 1.02 W/m^2 UV exposure (measured at a wavelength of 340 nm) under the following conditions:

- 58 min exposure – BST = 65 °C, ChT = 40 °C, RH = 40%;
- 2 min artificial rainfall with demineralized water and exposure BST = 40 °C, ChT = 25 °C;

Table 1. *Physical characteristics of manufactured PLA spun-bonded, non-woven fabrics.*

Stabilization temperature, °C	Mass surface, g/m^2 (c_v – coefficient of variation)
65	50.1 (5.3)
70	49.4 (4.1)
85	47.5 (2.2)
90	50.1 (1.1)
100	51.1 (0.5)
110	51.3 (0.7)

Table 2. Characteristic absorption bands of PLA observed under IR [19].

Band position, cm^{-1}	Chemical group	Material ordering, type of vibration
1752	C=O	Crystalline, stretching
1744	C=O	Amorphous, stretching
1450	CH_3	Asymmetric deformation
1380	CH_3	Symmetric deformation
1356	CH, CH_3	Crystalline, deformation and symmetric deformation
1265	COC + CH	Amorphous, stretching + deformation
1210	COC	Crystalline, stretching
1179	COC	Stretching
1125	CH_3	Rocking
1080	COC	Stretching

- 10 min with no exposure – BST = 30 °C, ChT = 20 °C, RH = 65%, for 42 h (where: BST - Black Standard Temperature, ChT - Chamber Air Temperature, and RH - Relative Humidity).

The weathering process simulating 3 seasons in a severer climate than temperate was denoted with symbol S3x2.

Test methods

After the artificial weathering process, the nonwovens were tested for shrinkage, a parameter that verifies their suitability for agricultural applications. Furthermore, the physical parameters and mechanical properties of the nonwovens were tested.

The following significant effects of nonwoven weathering were assessed:
- changes in the basic physical parameters: surface weight, m_p, apparent weight, ρ, thickness, air permeability and shrinkage;
- changes in directional mechanical properties: tensile strength, σ, and elongation at break, ε;
- changes in the nonwoven structure by analyzing changes in molecular and supermolecular structure by means of FTIR and WAXS techniques;

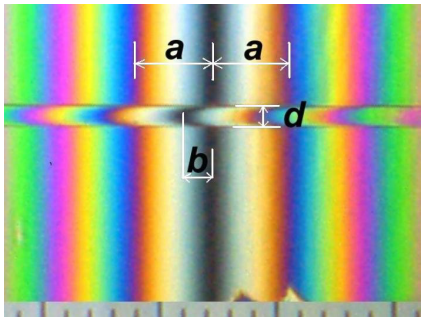

Figure 1. Example of the microscopic image of PLA fibers in the interference fringe field.

- changes in the total orientation of the nonwoven-forming polymer with the use of MPI microscopy;
- changes in the surface of the nonwoven-forming fibers by SEM microscopy.

Testing physical parameters

The physical parameters of nonwovens were determined according the standards for textiles: PN-EN 29073-1, 1994, Test methods for nonwovens – Determination of surface mass PN-EN ISO 9073-2, 2002, Test methods for nonwovens, part 2: Determination of thickness; PN-EN ISO 9073-3, 1994, Test methods for nonwovens; PN -EN ISO 9073-15, 2009, Test methods for nonwovens, Air permeability; PN-EN ISO 9073-3, 1994, Test methods for nonwovens, Determination of tensile strength and elongation.

Images of the nonwoven structure were observed by the high-vacuum technique by means of a JEOL JSM-5200LV microscope with the use of secondary electrons detector and backscattered electrons detector, at an accelerating voltage of 15 kV and magnifications and 5000×.

Changes in the dimensions of the nonwoven fabrics in hot air (in both the length and width directions) were determined in accordance with standard ISO 3759:2011: 'Textiles - Preparation, marking and measuring fabric specimens and garments in tests for the determination of dimensional change'. Shrinkage *S* of the non-woven fabrics was recorded as a percentage of the corresponding original value.

Testing the structure of the nonwoven-forming polymer

Absorption spectroscopy FTIR

The structure of the nonwoven-forming polymer was examined by IR spectroscopy using a FTIR-Nicolet 6700 spectrophotometer from Thermo Scientific, within the wavelength range of 4000 – 600 cm^{-1}, and a reflection attachment, type ITR, with a diamond crystal (Thermo Scientific). The FTIR spectra obtained in the system A = f(1/λ) were analyzed to assess changes in the intensity of absorption bands. The characteristics of the absorption bands of poly(lactic acid) are listed in ***Table 2***.

Wide angle X-ray scattering (WAXS)

The supermolecular structure of the nonwoven-forming polylactide was analyzed by means of the wide-angle X-ray scattering method. The diffraction profiles were obtained with Cu Kα (λ = 0.154 nm) by means of an X'Pert Pro X-ray diffractometer (from PANalytical) operating at 30 kV and 30 mA. The samples were studied in powder form. The content of crystalline material was determined from the following formula:

$$X_C = \frac{A_C}{A_C + A_A} \cdot 100\% \qquad (1)$$

where: A_A and A_C are calculated area under amorphous and crystalline curves, respectively.

Evaluating the orientation of nonwoven material (PLA)

The total orientation of the nonwoven material can be assessed by the determination of the optical birefringence index of fibers, Δ*n* [19]. Changes in this index are proportional to the orientation. The optical birefringence of fibers, Δ*n*, was calculated from the following formula:

$$\Delta n = \frac{b \cdot \lambda}{a \cdot d} \qquad (2)$$

where: λ = 0.55 μm – wavelength of white light, *a* – interfringe distance, *b* – deformation of zero fringe. The optical birefringence index was calculated as an average of 50 measurements of fibers.

Figure 1 shows the measurement principle of Δ*n* with the use of MPI3 microscope and CCD camera in the interference fringe field.

Scanning electron microscopy (SEM)

The surface images of the nonwoven-forming fibers were observed by means of a JEOL JSM-5200LV microscope by the high-vacuum technique using a secondary electrons detector and backscattered electrons detector, at an accelerating voltage of 15 kV and magnification 5000×.

Results and discussion

The weathering process of nonwovens resulted in their shrinkage that was dependent on the stabilization parameters used in calendering during the spunbonding process as well as on the artificial weathering conditions.

The shrinkage degrees of the nonwoven variants before and after the weathering process are listed in ***Table 3***.

The greatest shrinkage was observed in the case of nonwovens' (sample 1) treatment under the severest weathering conditions (S3x2): about 30% in the longitudinal direction and 50% in the transverse direction. Nonwovens Nos. 2 and 3 showed insignificant shrinkages. No shrinkage was shown by nonwovens Nos. 4, 5 and 6 stabilized at a temperature of 90 °C and higher regardless of the weathering conditions used.

Changes in the physical properties of the nonwoven samples before and after weathering are presented in ***Table 4.*** Samples before weathering were denoted with symbol '0'.

Changes in nonwoven surface mass, apparent density, thickness and air permeability observed are dependent on both the manufacturing and weathering conditions. The surface weight of most nonwoven variants increased after the weathering process. In the initial phase of this process up to 3 seasons of temperate climate (S3), the increase was small. During further weathering under simulated conditions of subtropical climate (S3x2), the surface mass increase was considerable: for sample No. 1 it was over threefold, for sample 2 – over 30%, for sample 3 – 7%, for sample 5 – 10% and for sample 6 – 2%. In the case of nonwoven No. 4, a small decrease in its surface weight was observed, practically insignificant from the point of view of its use.

Apparent density considerably decreased for all the variants of weathered nonwovens. The greatest changes in this parameter were observed for nonwoven No. 1. In the remaining cases of the nonwoven variants tested, their apparent density decreased by about 25% for samples stabilized at a temperature up to 90 °C, while it increased for nonwovens stabilized over this temperature.

During the weathering process the thickness of nonwovens increased. The most essential change in this parameter occurred in the case of nonwoven No. 1. The remaining samples showed an increase in thickness ranging from about 30% to about 80%.

The weathering process also brought about a decrease in the air permeability of nonwovens. Sample No. 1 showed that parameter decreased by more than four times. The air permeability values of samples 2 and 3 were changed by about 20% and 5%, respectively, while those of samples 4, 5 and 6 practically remained unchanged.

Table 5 presents changes in the mechanical properties of nonwovens depending on the stabilization temperature and the number of weathering seasons, some of which are illustrated in ***Figure 2***.

The values of breaking force in longitudinal and transverse directions of the nonwoven investigated increase with increasing the weathering time to assume an highest level for the stabilization variant at 90 °C. The strength of sample

Table 3. *Changes in the nonwoven dimensions before and after the weathering process.*

Sample No.	Stabilization temperature, °C	Number of weathering seasons	Initial dimensions, cm	Dimensions after weathering, cm	Shrinkage degree, %	
					Machine direction	Transverse direction
1	65	S1	75.0 × 32.0	74.0 × 31.5	1.3	1.6
		S3		74.0 × 31.5	1.5	1.8
		S3x2		50.5 × 13.0	32.7	59.4
2	70	S1		75.0 × 32.0	0	0
		S3		75.0 × 31.8		0.6
		S3x2		75.0 × 31.5		1.6
3	85	S1		75.0 × 32.0		0
		S3		75.0 × 31.8		0.6
		S3x2		75. 0 × 31.5		1.6
4	90	S1	75.0 × 37.5	75.0 × 37.5		
		S3	75.0 × 37.5	75.0 × 37.5		
		S3x2	75.0 × 37.5	75.0 × 37.5		
5	100	S1	75.0 × 32.0	75.0 × 32.0		0
		S3				
		S3x2				
6	110	S1				
		S3				
		S3x2				

Table 4. *Changes in the physical properties of nonwovens after weathering related to the values of the parameters of untreated nonwovens, for various calendering temperatures and exposure seasons.*

Sample No.	Stabilization temperature, °C	Number of weathering seasons, -	Surface mass, g/m^2	Apparent density, kg/m^3	Thickness, mm	Air permeability, dm^3/m^2*s
1	65	0	57.64	157.91	0.365	1008.0
		1	55.69	126.28	0.441	1109.0
		3	54.55	124.82	0.437	1159.0
		3x2	192.00	3.93	58.27	244.5
2	70	0	49.41	199.64	0.248	444.2
		3	50.92	146.74	0.347	544.6
		3x2	65.39	142.46	0.459	450.3
3	85	0	47.49	242.31	0.196	379.6
		3	49.73	189.79	0.262	366.6
		3x2	50.63	196.98	0.257	355.5
4	90	0	50.10	270.99	0.190	320.0
		3	49.50	249.84	0.200	322.0
		3x2	49.40	193.12	0.260	324.0
5	100	0	51.14	225.28	0.227	283.0
		3	51.99	217.53	0.239	287.9
		3x2	56.32	233.69	0.241	291.5
6	110	0	51.35	217.57	0.236	286.0
		3	51.76	230.04	0.225	297.9
		3x2	53.25	240.95	0.221	285.4

Table 5. *Changes in the mechanical properties of nonwovens from PLA 6251D after weathering related to the parameter values of initial nonwovens for various calendering temperatures and exposure seasons.*

Sample No.	Stabilization temperature, °C	Number of weathering seasons, -	Directional strength, N	
			Machine direction	Transverse direction
1	65	0	19.71	13.14
		1	16.48	12.88
		3	16.85	11.71
		3x2	-	-
2	70	0	53.04	26.02
		3	50.55	25.56
		3x2	51.23	24.52
3	85	0	69.91	35.48
		3	56.05	33.85
		3x2	61.25	31.64
4	90	0	76.02	53.29
		3	79.70	55.29
		3x2	77.78	52.55
5	100	0	56.89	35.47
		3	66.22	41.18
		3x2	62.47	36.93
6	110	0	35.41	29.16
		3	42.17	34.44
		3x2	46.17	39.84

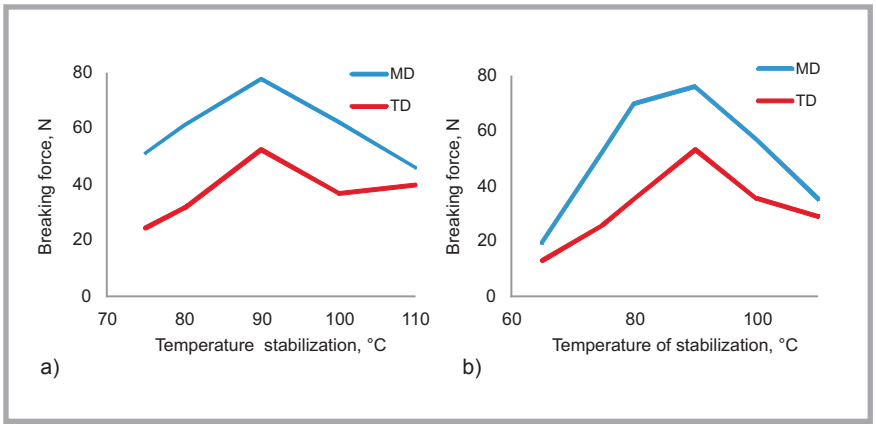

Figure 2. *Directional strengths of nonwovens - weathering variant S3x2 (a) compared with those of untreated nonwovens (b).*

No. 1 after weathering under severe conditions (S3x2) was not determined due to its high shrinkage that disqualifies it for anticipated agricultural applications.

Using FTIR spectrograms, the structural changes of the nonwoven polymer were qualitatively assessed on the basis of changes in the absorption peaks intensities correlated with corresponding chemical groups and the type of polymer ordering.

Subsequent figures show the spectrograms of weathered nonwovens (Nos. 1 and 4) in relation to those of untreated nonwovens. ***Figure 3*** shows examples of spectrograms illustrating changes in the nonwoven polymer structure (sample 1 – amorphous structure stabilized at 65 °C and sample 4 – semi-crystalline structure stabilized at 90 °C) depending on the weathering conditions.

In the spectrograms of weathered nonwovens, one can observe a new absorption band 1209 cm^{-1} (crystalline) for sample 1 calendered at a temperature of 65 °C and changes in the intensity of bands correlated with the structural rearrangement of the nonwoven polymer: doublet 1750 cm^{-1} (crystalline and amorphous), 1358 cm^{-1} (crystalline), 1269 cm^{-1} (amorphous) for the remaining samples.

The nonwovens stabilized at 70, 85, 90, 100 and 110 °C show the broadening and separation of band 1750 cm^{-1} (group C=O) into crystalline and amorphous, visible in the second derivative. The confirmation of increased polymer order of the nonwovens subjected to weathering is observed in spectrograms in the form of increased intensities of crystalline bands 1209 and 1358 cm^{-1}, and a decreased intensity of amorphous band 1269 cm^{-1}.

Changes in the structure of the nonwoven-forming polymer were examined by

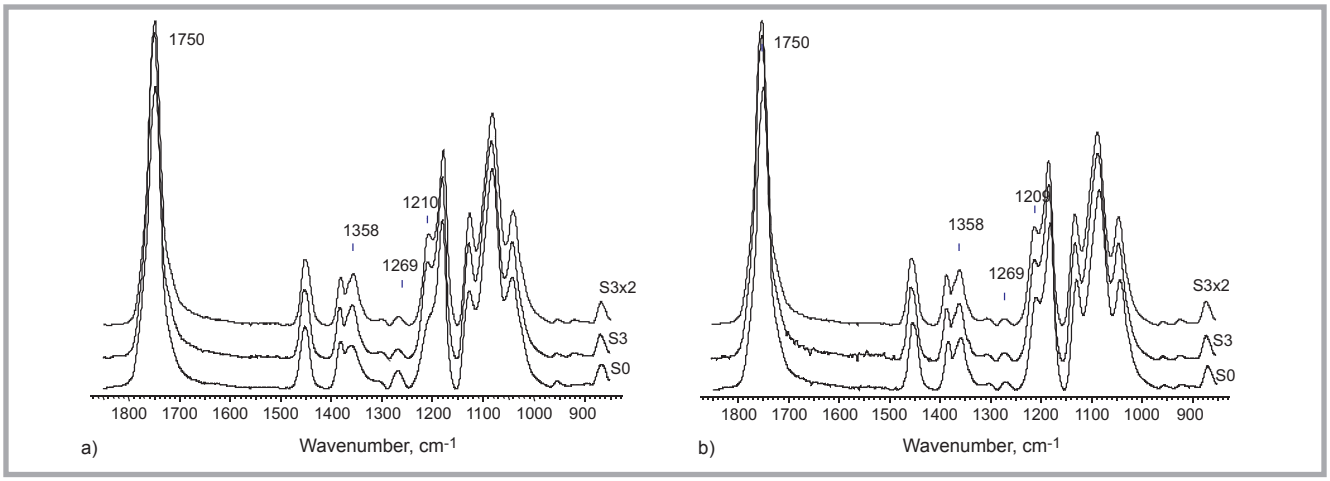

Figure 3. *FTIR spectrograms of nonwoven samples No. 1 (a) and 4 (b) depending on the weathering conditions.*

the WAXS technique to determine the degree of crystallinity, whose values for the nonwovens stabilized at various temperatures are listed in ***Table 6*** and illustrated in ***Figure 4***.

It was observed that the process of artificial weathering influenced the polymer structure of nonwovens stabilized under various thermal conditions. The greatest structural changes revealed by FTIR were observed in nonwoven No. 1 stabilized at 65 °C after weathering under the severest conditions (S3x2). The polymer of this nonwoven changes its ordering character from amorphous to semi-crystalline. In the case of nonwovens stabilized at higher temperatures, the absolute changes in the polymer structure determined as changes in the degree of crystallinity are not so clear. There was observed a high increase in the crystallinity degree at a temperature up to 90°C followed by its stabilization above this calendering temperature regardless of the weathering intensity.

Figures 5.a and ***5.b*** show qualitative changes in the structure of the nonwoven-forming polymer for nonwovens with different initial structures (samples 1 and 4) before and after weathering. In the case of amorphous nonwoven (sample 1), the weathering process causes the formation of crystalline structure. In the diffraction pattern, one can observe the appearance of a diffraction peak correlated with the crystallite plane 110/200. The ordering character of the polymer of nonwovens is changed from amorphous into semi-crystalline (***Figure 5.a***). The internal structure of the semi-crystalline polymer of nonwoven (sample 4) is developed to increase the crystalline areas as shown in ***Figure 5.b*** as an increase in the intensity of the diffraction peak correlated with the crystallite plane 110/200.

The more precise structural analysis of investigated samples was obtained by the deconvolution of the patterns into the amorphous halo and the crystalline peaks. For this analysis, the experimental data were fitted by a composite of the

Table 6. *Changes in the polymer crystallinity of nonwovens depending on their stabilization temperature and type of weathering.*

Sample No.	Stabilization temperature, °C	Type of weathering, -	Crystallinity degree, %
1	65	0	2
		S3	2
		S3x2	35
2	70	S0	8
		S3	9
		S3x2	37
3	85	S0	38
		S3	43
		S3x2	46
4	90	S0	46
		S3	46
		S3x2	49
5	100	S0	46
		S3	50
		S3x2	50
6	110	S0	54
		S3	49
		S3x2	51

Gauss and Lorentz functions calculated using the WAXSFIT software [20] based on Hindeleh and Johnson's method. The shapes of the amorphous halo and the

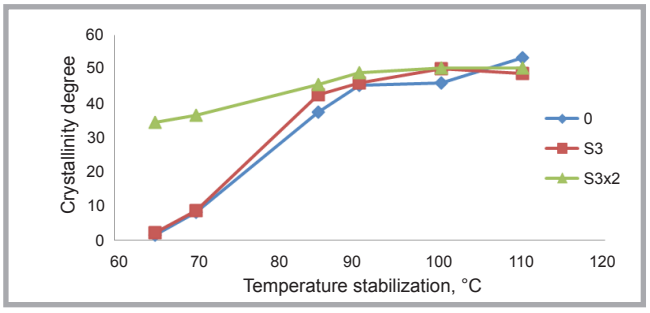

Figure 4. *Change in the polymer crystallinity of nonwovens before and after weathering.*

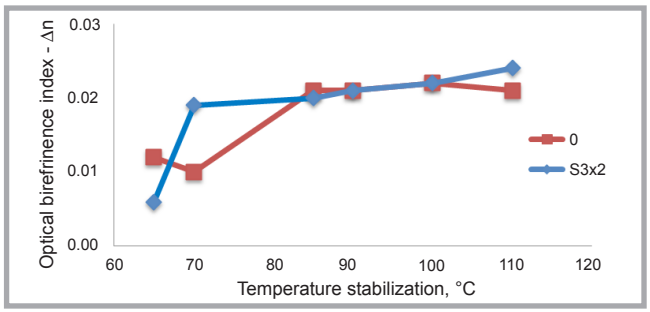

Figure 6. *Changes in the optical anisotropy of the polymers of initial and weathered nonwovens.*

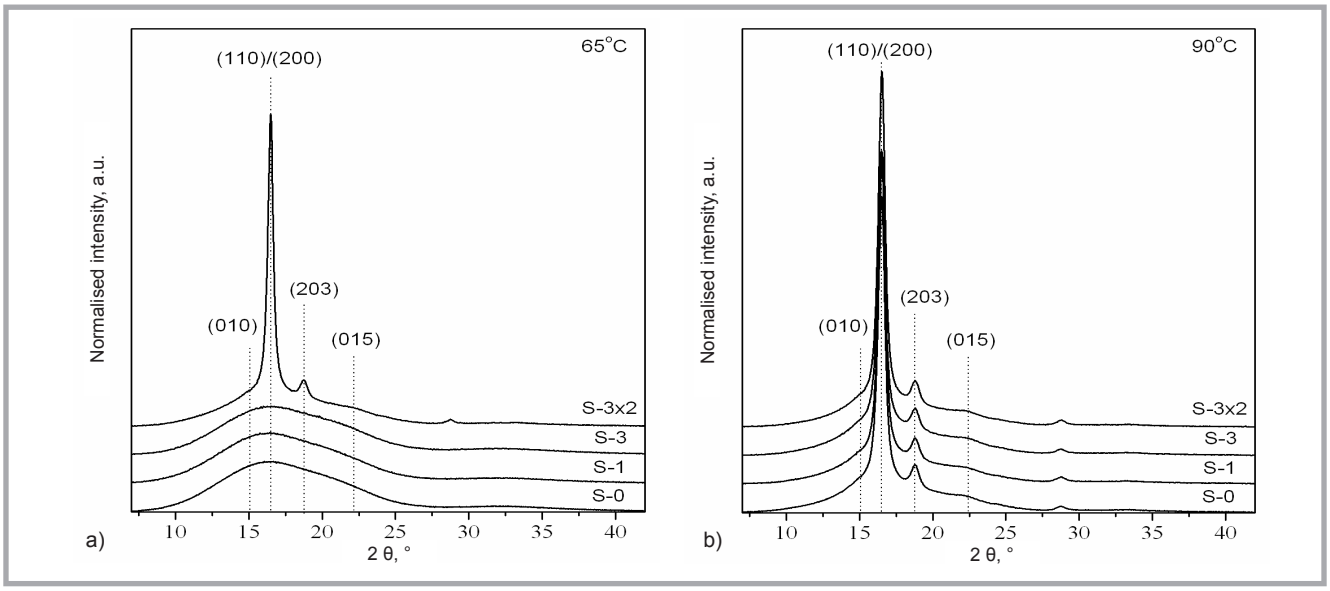

Figure 5. *WAXS diffraction patterns of nonwovens 1(a) and 4 (b) depending on the weathering conditions*

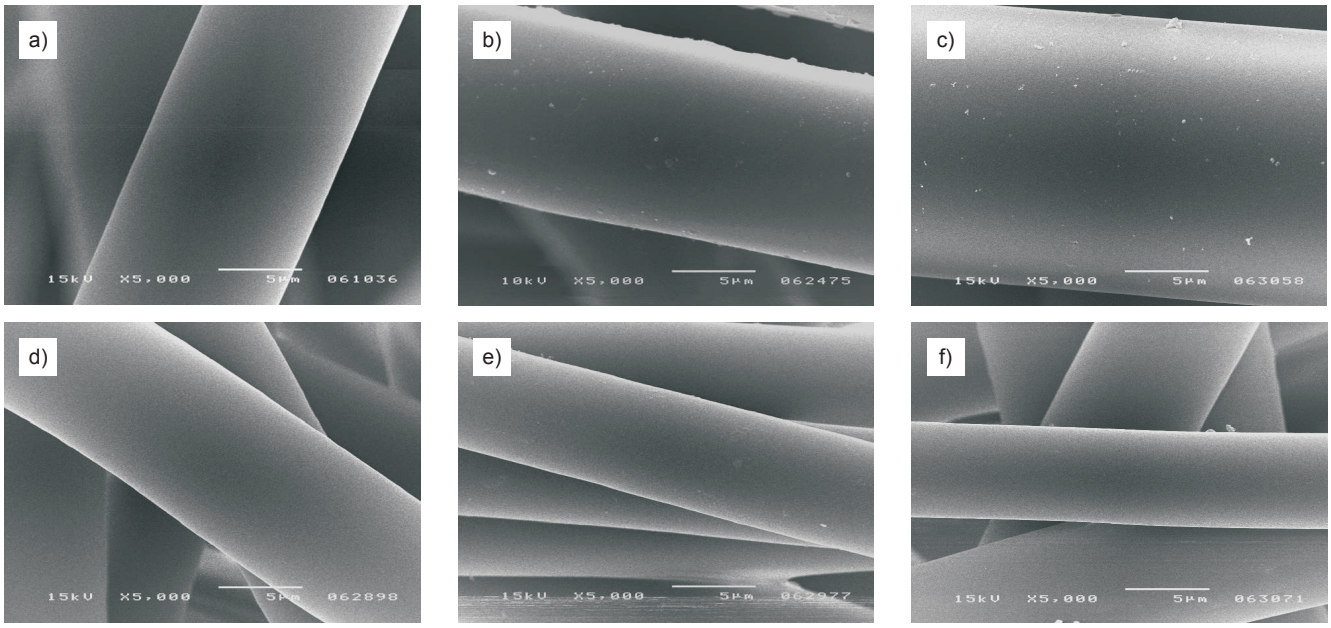

Figure 7. *SEM images of nonwovens stabilized at 65 and 90 °C (samples 1 and 4) after weathering compared to those of initial nonwovens. Sample No. – Weathering variant: a) 24, b) 24 S3, c) 24 S3x2, d) 49, e) 49 S3, f) 49 S3x2.*

mesomorphic and crystalline peaks were selected according to the model proposed by Stoclet et al. [21].

The optical birefringence index, Δn, well characterizes the total orientation of the polymer of nonwoven. Changes in this index are proportional to this orientation [22].

Figure 6 presents changes in the optical birefringence of the nonwoven-forming polymer, indirectly characterizing the total orientation of the polymer.

The optical birefringence index, Δn, of the polymer of initial nonwovens considerably changes for samples 1 and 2 stabilized at 65 and 70 °C. The increase in the stabilization temperature of nonwovens up to 90 and 100 °C causes a small increase in optical birefringence, assuming then a constant value, $\Delta n = 0.022$, indicating polymer stabilization. The weathering of nonwovens calendered at lower temperatures considerably changes the value of this index, while in the case of higher calendering temperatures, its values remains at a constant level, indicating a stable orientation of the polymer and its small sensibility to the artificial weathering process used. Assessing the changes in the structure of nonwovens on the basis on changes in the intensity of characteristic absorption bands, determined by FTIR, and changes in the degree of crystallinity determined by WAXS as well as in the polymer orientation evaluated by the method of optical microscopy, it has been found that a stable structure of the nonwoven-forming polymer can be obtained by the thermal treatment of the nonwovens performed at a temperature at least of 90 °C.

Changes in the surface of the nonwoven-forming fibers subjected to weathering in relation to those of initial nonwovens are illustrated, as an example, by SEM images presented in ***Figure 7***.

On the surface of the nonwoven-forming fibers, one can observe pointwise existing damages resulted from a longer and more intensive weathering.

Conclusions

Based on the investigations performed, one can draw the following conclusions:

- In relation to initial samples (unweathered):
  The stabilization of PLA 6251D spunbonded nonwovens on a calender within the temperature range used decisively affects their physical features and mechanical properties. Along with temperature increase the apparent density of the nonwovens increases, while their thickness and air permeability decrease. As far as mechanical properties are concerned, it has been found that the directional strengths of nonwovens clearly increase with increasing their stabilization temperature to reach the temperature of 90 °C. The stabilization process of nonwovens within the temperature range used influences their internal structure. The calendering process of nonwovens results in the development of an optimal crystalline structure of the nonwoven-forming polymer [23].
- In relation to samples subjected to artificial weathering:
  It has been found that there is a limiting temperature of stabilization; after exceeding it, nonwovens do not shrink in the weathering process carried out even under severe conditions, and the mechanical properties of nonwovens assume highest values. The nonwoven stabilized at the lowest temperature (65 °C), shrinks already after a single season-weathering, and under severe weathering conditions, its shrinking degree disqualifies it from use under environmental conditions.

  The mechanical properties of the nonwovens investigated, assessed for particular variants of weathered samples, are changed to a significant extent. As a rule, the values of directional strengths increase up to the most beneficial level for the calendering variant at a temperature of 90 °C.

  The highest strength values with no shrinkage, even under severe weathering conditions, are shown by the nonwoven calendered at a temperature of 90 °C. This results from the optimally developed internal structure of

the nonwoven-forming polymer. Thus one may use it, in agricultural applications, under environmental conditions during a strong sun exposure, maintaining the stability and immutability of its properties within an intended period of exploitation.

Acknowledgment

The research work presented has been performed within the framework of the key project titled „Biodegradable fibrous products" (acronym: Biogratex) supported by European Regional Development Fund; Agreement No. POIG.01.03.01-00-007/08-00.

References

1. Engleberg I, Kohn J. *Biomaterials* 1991; 12: 292.
2. Kulkarni R, Pani K, Newman C, Leonard F. *Arch Surg* 1966; 93: 839.
3. Cutright DE, Beasley JD, Perez B. *Oral Surg* 1971; 232:165.
4. Hofman AS. *J Appl Polym Sci*: *Appl Polym Symp* 1977; 31: 313.
5. Lenslag JW, Pennongs AJ, Bos RRM, Rozema FR, Boering G.: *Biomaterials* 1987; 8: 70.
6. Zislis T, Mark DE, Cerbas EL, Hollinger JO. *J Oral Implantol* 1989; 15: 167.
7. Cohen S, Yoshioka T, Lucarelli M, Hwang LH, Langer R. *Pharm Res* 1991; 8: 713.
8. Coombes AGA, Yeh MK, Lavelle EC, Davis SS. *J Controlled Release* 1998; 52: 311.
9. Park TG, Lu WQ, Crotts G. *J Controlled Release* 1995; 33: 211.
10. Peter SJ, Miller MJ, Yasko AW, Yaszemski MJ, Mikos AG. *J Biomed Mater Res* 1998; 43: 422.
11. Freed LE, Gordana VN, Langer R. *BioTechnology* 1994; 12: 689.
12. Vert M. *Angew Makromol Chem* 1989; 166: 8.
13. Couvreur P, Puisieux F. *Adv Drug Delivery Rev* 1993; 10: 62.
14. Langer R. *Chem Eng Commun* 1980; 6: 48.
15. Foltynowicz Z, Jakubiak P. *Polimery* 2002; 11-12: 769.
16. Rafael A. Auras et all. *Poly(Lactic Acid): Synthesis, Structures, Properties, Processing, and Applications*, John Wiley & Sons, 2010.
17. Krucińska I, Strzembosz W, Majchrzycka K, Brochocka A, Twarowska-Schmidt K, Sulak K. *Fibres & Textiles in Eastern Europe* 2012; 6B(96): 77-83.
18. Pluta M, Murariu M, Alexandre M, Galeski A, Dubois P, *Polymer Degradation and Stability* 2008; 93: 925.
19. Furukawa T, Sato H, Murakami R, Zhang J, Duan Y, Noda I, Ochiai S, Ozaki Y. *Macromolecules* 2005; 38: 15.
20. Rabiej M, Rabiej S. *Analiza rentgenowskich krzywych dyfrakcyjnych polimerów za pomocą programu komputerowego WAXSFIT*, Bielsko-Biała: ATH Press, 2006.
21. Stoclet G, Seguela R, Lefebvre J-M and Rochas C. New insights on the strain-induced mesophase of poly(D,L-lactide): in situ WAXS and DSC study of the thermomechanical stability. *Macromol* 2010, 43: 7228-7237.
22. Read BE, Duncan JC, Meyer DE. *Polymer Testing* 1984; 4: 143.
23. Puchalski M, Krucinska I, Sulak K, Chrzanowski M, Wrzosek H. *Journal of Applied Polymer Science* 2013; (art. no. TRJ-12-0388).

Received 01.08.2012 ***Reviewed 11.12.2012***